NJC

PAPER

View Article Online
View Journal | View Issue

Cite this: *New J. Chem.*, 2018, **42**, 19644

Extending the family of quinolone antibacterials to new copper derivatives: self-assembly, structural and topological features, catalytic and biological activity†

Panagiotis Xerras,[a] Anna-Maria Bacharidou,[b] Stavros Kalogiannis,[b] Franc Perdih,[c] Marina V. Kirillova,[d] Alexander M. Kirillov,*[de] Iztok Turel*[c] and George Psomas*[a]

A new series of copper(II) compounds, $[Cu(pef)_2(MeOH)]$ (**1**), [Cu(pef)(bipyam)Cl] (**2**), [Cu(pef)(phen)Cl] (**3**) and [Cu(pef)(bipy)Cl] (**4**), bearing the quinolone family member pefloxacin (Hpef) were self-assembled in the presence (optional) of N,N′-donor heterocyclic ligands such as 2,2′-bipyridylamine (bipyam), 1,10-phenanthroline (phen), or 2,2′-bipyridine (bipy). The products were fully characterized, including single-crystal X-ray diffraction analysis of **2–4**. The structures are extended into 1D (**2**), 2D (**3**), or 3D (**4**) networks *via* multiple H-bonds between the monocopper(II) units and guest water and/or methanol molecules; the latter are arranged into different types of water and hybrid water–methanol clusters. The resulting H-bonded networks were classified from a topological viewpoint, revealing diverse topologies that also include an undocumented type. Compounds **2–4** also act as homogeneous catalysts in a model oxidation reaction, namely the mild oxidation of C_6–C_8 cycloalkanes by H_2O_2 at 50 °C to give cyclic alcohols and ketones. The effects of various reaction parameters (substrate scope, temperature, and loadings of catalyst, cycloalkane, and oxidant) and selectivity features were investigated. Besides, products **1–4** also show remarkable antibacterial activity against four different microorganisms (*Escherichia coli*, *Xanthomonas campestris*, *Staphylococcus aureus* and *Bacillus subtilis*), which is superior to that of free Hpef. The interaction of the Cu(II) compounds with calf-thymus DNA was studied suggesting intercalation as the most possible binding mode. Furthermore, the interaction of the obtained copper(II) derivatives with human/bovine serum albumin was investigated by fluorescence emission spectroscopy and the corresponding albumin-binding constants were established. This study widens a limited family of transition metal pefloxacin derivatives.

Received 21st October 2018,
Accepted 2nd November 2018

DOI: 10.1039/c8nj05338c

rsc.li/njc

Introduction

Pefloxacin (Hpef, Fig. 1) is a synthetic antimicrobial agent belonging to the group of quinolones which are well established and frequently used antibacterial agents studied in many fields.[1,2] In particular, two examples of such fields concern environmental impact[3] and toxicity that may cause side-effects[4] which may both be connected with metal ion interactions. Magnesium ions are crucial for the antibacterial activity of quinolones,[5] but, on the other hand, complexes of other metals were reported to exert other types of biological activity, for example cytotoxicity.[6] Moreover, it was also reported that iron chelation by fluoroquinolones leads to epigenetic effects through inhibition of alpha-ketoglutarate-dependent dioxygenases that require iron as a co-factor.[7] In the mechanism of cellular death induced by quinolones, leaching of iron from iron–sulfur clusters and the stimulation of the Fenton reaction also take place.[8] Although it is difficult to study the

[a] *Department of General and Inorganic Chemistry, Faculty of Chemistry, Aristotle University of Thessaloniki, GR-54124 Thessaloniki, Greece. E-mail: gepsomas@chem.auth.gr*
[b] *Department of Nutrition and Dietetics, Faculty of Agriculture, Food Technology and Nutrition, Alexander Technological Educational Institution, Sindos, Thessaloniki, Greece*
[c] *Faculty of Chemistry and Chemical Technology, University of Ljubljana, Vecna pot 113, 1000 Ljubljana, Slovenia. E-mail: Iztok.Turel@fkkt.uni-lj.si*
[d] *Centro de Química Estrutural, Instituto Superior Técnico, Universidade de Lisboa, Av. Rovisco Pais, 1049-001, Lisbon, Portugal. E-mail: kirillov@tecnico.ulisboa.pt*
[e] *Peoples' Friendship University of Russia (RUDN University), 6 Miklukho-Maklay st., Moscow, 117198, Russian Federation*

† Electronic supplementary information (ESI) available: Experimental protocols for biological studies; tables with crystallographic data and selected bonding parameters; the albumin constants; comparison of the biological activity; additional figures containing fluorescence emission UV-vis spectra and other data; and crystallographic CIF files for **2–4**. CCDC 1844910–1844912. For ESI and crystallographic data in CIF or other electronic format see DOI: 10.1039/c8nj05338c

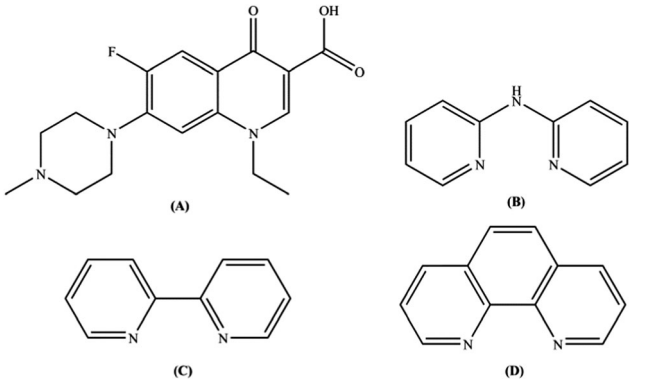

Fig. 1 The syntax formula of (A) Hpef, (B) bipyam, (C) bipy and (D) phen.

behavior of metal complexes under biological conditions, such information would be very important for understanding the bioactivity of pefloxacin derivatives. As a second-generation quinolone, Hpef is active against a broad spectrum of Gram-(−) and Gram-(+) bacteria.[9] With regard to coordination compounds, limited examples of Ag,[10] Mn,[11] and Zn[12] complexes with pefloxacin were structurally characterized among those reported.[13–16] With particular regard to copper, some Cu pefloxacin derivatives were described;[14,15] however, these studies do not report the X-ray single-crystal structures of the obtained compounds.

Copper is a d-block element that is essential for life but can also be toxic, depending upon the concentration.[17] It has unique properties and is specifically needed in a number of enzymes, especially those important for redox processes.[18,19] Copper is the strongest Lewis acid in Group 11 of the periodic table and has the ability to mediate electron transport by accepting and donating electrons. It took a long time to understand the nature and role of copper–oxygen intermediates within copper-containing enzymes and abiological catalysts.[20] The formation of highly reactive hydroxyl radicals ($OH^{\bullet}$) in a Fenton-type reaction can also be promoted by copper.[21] Sigman and coworkers reported the first copper complex $[Cu(phen)_2]^+$ (phen = 1,10-phenantroline) that shows efficient DNA cleavage activity.[22,23] Other copper(II) derivatives that can oxidatively cleave DNA under physiological conditions were later prepared. Frequently such complexes require a reducing agent and hydrogen peroxide (or dioxygen) for their activity.

The copper-quinolone derivatives are the most popular metal complexes of quinolones and have been thoroughly studied.[24,25] Examples reported so far include copper derivatives with the first-generation quinolones, such as flumequine,[26] nalidixic acid[27] and oxolinic acid,[28] the second-generation, such as cinoxacin,[29] ciprofloxacin,[30–32] enrofloxacin,[33] norfloxacin[34,35] and ofloxacin,[29,36] and the third-generation such as gatifloxacin[37] and sparfloxacin.[38] Most of these complexes have been structurally characterized showing in most cases a four- or a five-coordinate environment around copper.

The development of abiological catalysts that can function in biological systems and so-called bioorthogonal chemistry are the hot research topics in recent years which clearly show the prospective catalytic applications of metal complexes.[39–44] However, catalytic properties of metal–quinolone derivatives remain largely unstudied. Hence, one of the aims of the present work consisted of exploring the oxidation catalytic potential of new copper pefloxacin derivatives. The conditions used in our experiments are definitely far from physiological conditions and it would be an oversimplification to suggest that such reactions occur in the human body. However, we believe it is worth obtaining more information on the catalytic properties of metal–drug complexes and also about their potential roles in living systems. It could not be excluded that certain reactions in which metal complexes might be involved (which were not extensively studied) may also be related to various effects, *e.g.* toxicity.

Herein, we present the synthesis and detailed characterization of a new series of copper(II) compounds derived from the second-generation quinolone pefloxacin in the presence (optional) of 2,2′-bipyridinylamine (bipyam), 1,10-phenanthroline (phen), and 2,2′-bipyridine (bipy) as N-donor co-ligands (Fig. 1(B)–(D)). Four compounds were isolated and formulated as $[Cu(pef)_2(MeOH)]$ for **1** and $[Cu(pef)(L)Cl]$ (L = bipyam, phen or bipy) for **2–4**, respectively. The characterization of **1–4** was achieved by standard physicochemical and spectroscopic techniques, as well as by single-crystal X-ray diffraction. Hence, compounds **2–4** represent unique examples of structurally characterized Cu pefloxacin derivatives. In addition, products **1–4** were screened as homogeneous catalysts for the mild oxidation of C_6–C_8 cycloalkanes as model substrates to give the corresponding cyclic alcohols and ketones. The *in vitro* biological activity of **1–4** was also investigated in detail, including: (a) the evaluation of their antimicrobial activity against four Gram-positive or Gram-negative microorganisms (*i.e.*, *Escherichia coli* NCTC 29212 (*E. coli*), *Xanthomonas campestris* ATCC 1395 (*X. campestris*), *Staphylococcus aureus* ATCC 6538 (*S. aureus*) and *Bacillus subtilis* ATCC 6633 (*B. subtilis*)); (b) the investigation of their binding to bovine (BSA) and human (HSA) serum albumins; (c) the determination of their binding mode and the binding strength to calf-thymus (CT) DNA; and (d) the investigation of their binding competition with the well-known DNA-intercalator ethidium bromide (EB).

Experimental

Materials, instrumentation and physical measurements

The reagents $CuCl_2{\cdot}2H_2O$, pefloxacin, bipy, phen, bipyam, KOH, NaCl, CT DNA, EB, BSA, HSA, and trisodium citrate were purchased from Sigma-Aldrich Co, and all solvents were purchased from ChemLab. All the chemicals and solvents were reagent grade and were used as purchased without any further purification. DNA stock solution was prepared by dilution of CT DNA in buffer (containing 15 mM trisodium citrate and 150 mM NaCl at pH 7.0) followed by exhaustive stirring for three days, and kept at 4 °C for no longer than a week. The stock solution of CT DNA gave a ratio of UV absorbance at 260 and 280 nm (A_{260}/A_{280}) of 1.90, indicating that the DNA was sufficiently free of protein contamination.[45] The DNA concentration was determined

by the UV absorbance at 260 nm after 1:20 dilution using ε = 6600 M^{-1} cm^{-1}.[46]

Infrared (IR) spectra (400–4000 cm^{-1}) were recorded on a Nicolet FT-IR 6700 spectrometer with samples prepared as KBr disks. UV-visible (UV-vis) spectra were recorded as nujol mulls and in solution at concentrations in the range 1×10^{-5}–5×10^{-3} M on a Hitachi U-2001 dual beam spectrophotometer. Room temperature magnetic measurements were carried out by the Faraday method. C, H and N elemental analyses were performed on a Perkin-Elmer 240B elemental analyzer. Molar conductivity measurements were carried out with a Crison Basic 30 conductometer. Fluorescence spectra were recorded in solution on a Hitachi F-7000 fluorescence spectrophotometer. Viscosity experiments were carried out using an ALPHA L Fungilab rotational viscometer equipped with an 18 mL LCP spindle and the measurements were performed at 100 rpm. For the analysis of the reaction mixtures in catalytic tests, gas chromatography (GC) analyses were run on an Agilent Technologies 7820A series gas chromatograph (He as the carrier gas) equipped with an FID detector and BP20/SGE (30 m × 0.22 mm × 0.25 μm) capillary column.

Synthesis of the compounds

Synthesis of [Cu(pef)$_2$(MeOH)], 1. Pefloxacin (0.5 mmol, 166 mg) was dissolved in methanol (10 mL) and deprotonated by KOH (0.5 mmol, 0.5 mL 1 M). After 30 min stirring, the initial solution was added to a methanolic solution (5 mL) of $CuCl_2{\cdot}2H_2O$ (0.25 mmol, 43 mg). The reaction mixture was stirred for 30 min and left for slow evaporation. A green-blue precipitate of [Cu(pef)$_2$(MeOH)], **1** (150 mg, 75%), was collected after two weeks. Anal. calcd for [Cu(pef)$_2$(MeOH)], $C_{35}H_{42}CuF_2N_6O_7$ (M_W = 760.30): C 55.29, H 5.57, N 11.05%; found: C 55.12, H 5.45, N 10.75%. IR (KBr disk): ν_{max}/cm^{-1}: ν(C=O)$_{pyridone}$, 1633 (very strong (vs)); $\nu_{asym}(CO_2)$, 1598 (vs); $\nu_{sym}(CO_2)$, 1372 (strong (s)); $\Delta\nu(CO_2) = \nu_{asym}(CO_2) - \nu_{sym}(CO_2)$ = 226 cm^{-1}. UV-vis: as nujol mull, λ/nm: 740, 335, 310; in DMSO, λ/nm (ε/M^{-1} cm^{-1}): 735(75), 332(11 500), 315(14 500). μ_{eff} = 1.84 BM at room temperature. The complex is soluble in DMF and DMSO (Λ_M = 8 S cm^2 mol^{-1}, 1 mM DMSO solution).

Synthesis of [Cu(pef)(L)Cl], 2–4 (L = bipyam for 2, phen for 3, and bipy for 4). Complexes **2–4** were prepared in a similar way with the use of the corresponding N,N′-donor ligand. More specifically, a methanolic solution (20 mL) of Hpef (0.25 mmol, 83 mg) and KOH (0.25 mmol, 14 mg) was stirred for 30 min and then added, simultaneously with a methanolic solution (5 mL) of the corresponding N,N′-donor (0.25 mmol), to a methanolic solution (5 mL) of $CuCl_2{\cdot}2H_2O$ (0.25 mmol, 43 mg). The obtained reaction mixture was stirred for 20 min and left for slow evaporation.

[Cu(pef)(bipyam)Cl]·2H$_2$O, 2·2H$_2$O. Bipyam (0.25 mmol, 43 mg) was used as the N,N′-donor. Dark green crystals of [Cu(pef)(bipyam)Cl]·2H$_2$O, **2**·2H$_2$O (105 mg, yield: 70%), suitable for X-ray structure determination, were collected after three weeks. Anal. calcd. for [Cu(pef)(bipyam)Cl]·2H$_2$O, $C_{27}H_{32}ClCuFN_6O_5$ (M_W = 638.58): C 50.78, H 5.05, N 13.16%; found: C 50.92, H 4.89, N 12.82%. IR (KBr disk): ν_{max}/cm^{-1}: ν(C=O)$_{pyridone}$, 1639 (vs); $\nu_{asym}(CO_2)$, 1586 (vs); $\nu_{sym}(CO_2)$, 1380 (s); $\Delta\nu(CO_2)$ = 206 cm^{-1}; ρ(C–H)$_{bipyam}$: 769 (m). UV-vis: as nujol mull, λ/nm: 735, 331, 313; in DMSO, λ/nm (ε/M^{-1} cm^{-1}): 730(125), 335(sh) (7500), 316(17 000). μ_{eff} = 1.78 BM at room temperature. The complex is soluble in MeOH, EtOH, DMF and DMSO (Λ_M = 7 S cm^2 mol^{-1}, 1 mM DMSO solution) and partially soluble in H_2O.

[Cu(pef)(phen)Cl]·MeOH·2H$_2$O, 3·MeOH·2H$_2$O. Phen (0.25 mmol, 45 mg) was used as the N,N′-donor. Dark green well-formed crystals of [Cu(pef)(phen)Cl], **3** (130 mg, yield: 85%), suitable for X-ray structure determination, were collected after ten days. Anal. calcd. for [Cu(pef)(phen)Cl]·MeOH·2H$_2$O, $C_{30}H_{35}ClCuFN_5O_6$ (M_W = 679.62): C 53.02, H 5.19, N 10.31%; found: C 52.84, H 4.97, N 10.57%. IR (KBr disk): ν_{max}/cm^{-1}: ν(C=O)$_{pyridone}$, 1631 (vs); $\nu_{asym}(CO_2)$, 1613 (vs); $\nu_{sym}(CO_2)$, 1376 (s); $\Delta\nu(CO_2)$ = 237 cm^{-1}; ρ(C–H)$_{phen}$: 725 (m). UV-vis: as nujol mull, λ/nm: 670, 331, 313; in DMSO, λ/nm (ε/M^{-1} cm^{-1}): 685 (60), 327 (sh) (10 900), 316(12 500). μ_{eff} = 1.79 BM at room temperature. The complex is soluble in MeOH, EtOH, DMF and DMSO (Λ_M = 10 S cm^2 mol^{-1}, 1 mM DMSO solution).

[Cu(pef)(bipy)Cl]·0.5MeOH·4H$_2$O, 4·0.5MeOH·4H$_2$O. Bipy (0.25 mmol, 39 mg) was used as the N,N′-donor. Dark green well-formed crystals of [Cu(pef)(bipy)Cl]·0.5MeOH·4H$_2$O, **4**·0.5MeOH·4H$_2$O (110 mg, yield: 75%), suitable for X-ray structure determination, were collected after two weeks. Anal. calcd for [Cu(pef)(bipy)Cl]·0.5MeOH·4H$_2$O, $C_{27.5}H_{37}ClCuFN_5O_{7.5}$ (M_W = 675.21): C 48.89, H 5.52, N 10.37%; found: C 48.75, H 5.38, N 10.69%. IR (KBr disk): ν_{max}/cm^{-1}: ν(C=O)$_{pyridone}$, 1632 (vs); $\nu_{asym}(CO_2)$, 1609 (vs); $\nu_{sym}(CO_2)$, 1388 (s); $\Delta\nu(CO_2)$ = 221 cm^{-1}; ρ(C–H)$_{bipy}$, 775 (medium (m)). UV-vis: as nujol mull, λ/nm: 675, 332, 311; in DMSO, λ/nm (ε/M^{-1} cm^{-1}): 685 (30), 330 (shoulder (sh)) (8900), 313(13 200). μ_{eff} = 1.98 BM at room temperature. The complex is soluble in MeOH, EtOH, DMF and DMSO (Λ_M = 6 S cm^2 mol^{-1}, in 1 mM DMSO solution) and partially soluble in H_2O.

X-ray crystal structure determination

Single-crystal X-ray diffraction data were collected on an Agilent Technologies SuperNova Dual diffractometer using Mo-Kα radiation (λ = 0.71073 Å) at room temperature (**2**·2H$_2$O and **4**·0.5MeOH·4H$_2$O) and at 150 K (**3**·MeOH·2H$_2$O). The data were processed using CrysAlis Pro.[47] The structures were solved by direct methods and refined by a full-matrix least-squares procedure based on F^2 with SHELX-97.[48] All the non-hydrogen atoms were refined anisotropically. Hydrogen atoms were readily located in difference Fourier maps and were subsequently treated as riding atoms in geometrically idealized positions with $U_{iso}(H) = kU_{eq}$(C or O), where k = 1.5 for hydroxyl and methyl groups, which were permitted to rotate but not to tilt, and 1.2 for all other H atoms unless otherwise noted. In the crystal structure **2**·2H$_2$O, hydrogen atoms bonded to water solvate molecules O4 and O5 and to bipyam amino atom N3 were refined restraining the bonding distances with $U_{iso}(H) = 1.5U_{eq}(O)$ and $U_{iso}(H) = 1.2U_{eq}(N)$. In the crystal structure **3**·MeOH·2H$_2$O, hydrogen atoms bonded to water solvate molecules O4 and O5 were refined freely with $U_{iso}(H) = 1.5U_{eq}(O)$. In the crystal structure **4**·0.5MeOH·4H$_2$O, hydrogen atoms bonded to water solvate molecules O7–O14 were refined restraining the bonding distances with $U_{iso}(H) = 1.5U_{eq}(O)$. Crystallographic data are listed in Table S1 (ESI†).

Topological analysis

Topological analysis of H-bonded networks was carried out using Topos software and following the concept of the simplified underlying net.[49–52] Such underlying nets were generated by contracting Cu molecular units and water or water–methanol aggregates to the corresponding centroids, maintaining their connectivity *via* hydrogen bonds. Only strong D–H···A hydrogen bonds were considered, wherein H···A < 2.50 Å, D···A < 3.50 Å, and ∠(D–H···A) > 120°; D and A stand for donor and acceptor atoms.[49,50] The obtained nets were then classified from the topological viewpoint.

Mild catalytic oxidation of alkanes

Alkane oxidation reactions were typically performed in air atmosphere in thermostated glass reactors equipped with a condenser under vigorous stirring at 50 °C and using MeCN as the solvent (up to 2.5 mL total volume). In a typical experiment, copper(II) catalyst (5.0 μmol) and gas chromatography (GC) internal standard ($MeNO_2$, 25 μL) were introduced into MeCN solution, followed by addition of an alkane substrate (1 mmol). The reaction started upon introduction of hydrogen peroxide (50% in H_2O, 5 mmol) in one portion. The oxidation reactions were monitored by withdrawing small aliquots after different periods of time, which were treated with PPh_3 for the reduction of remaining H_2O_2 and alkyl hydroperoxides that are typically formed as primary products in alkane oxidations.[53,54] The samples were then analyzed by GC using nitromethane as an internal standard. The formation of alkyl hydroperoxides as primary intermediate products was also confirmed by GC analyses of the reaction mixtures before and after the treatment with PPh_3 (Shul'pin's method).[53,54] Attribution of peaks was made by comparison with chromatograms of authentic samples. Blank tests confirmed that alkane oxidations do not proceed in the absence of copper catalyst. Compound **1** was also tested and found to be inactive in the present type of catalytic reactions, resulting in negligible yields of products (<1%). The inactivity of **1** can be explained by its quick degradation in the course of catalytic experiments.

Biological activity studies

In order to study *in vitro* the biological activity of Hpef and its complexes **1–4** (*i.e.*, antimicrobial activity and interaction with DNA or albumins), they were initially dissolved in DMSO (1 mM). Mixing of such solutions with the aqueous buffer DNA solutions used never exceeded 5% DMSO (v/v) in the final solution, which was needed due to low aqueous solubility of most compounds.

The antimicrobial activity of the compounds was evaluated by determining the MIC values toward two Gram-(−) (*E. coli* and *X. campestris*) and two Gram-(+) (*S. aureus* and *B. subtilis*) bacterial species. The albumin binding studies were performed by tryptophan fluorescence quenching experiments. The interaction of the compounds with CT DNA was investigated by UV-vis spectroscopy and viscosity measurements and *via* the evaluation of the EB-displacing ability of the complexes studied by fluorescence emission spectroscopy. Detailed procedures regarding the study of the biological activity of the compounds are given in the ESI† (Sections S1–S5).

Results and discussion

Synthesis and physicochemical characterization

Compounds **1–4** were synthesized in good yield *via* the self-assembly reaction of pefloxacin, deprotonated by KOH, with $CuCl_2{\cdot}2H_2O$ in the absence (reaction (1) for **1**) or presence of the corresponding N,N′-donor co-ligand (L = bipy, phen, and bipyam for **2–4**, respectively; reaction (2)):

$$CuCl_2{\cdot}2H_2O + 2Hpef + 2KOH + MeOH \rightarrow [Cu(pef)_2(MeOH)] + 2KCl + 4H_2O \quad (1)$$

$$CuCl_2{\cdot}2H_2O + Hpef + KOH + L \rightarrow [Cu(pef)(L)Cl] + KCl + 3H_2O \quad (2)$$

Products **1–4** were characterized by elemental analysis, IR and UV-vis spectroscopies and magnetic measurements at room temperature. The structures of **2–4** were determined by X-ray crystallography. The complexes are mainly soluble in DMSO and DMF and partially in organic solvents, while they remain insoluble in H_2O. For the biological experiments, the compounds were initially dissolved in DMSO (1 mM); thereafter a solution of the complexes in a mixture of DMSO : water (5% in DMSO) was used. The values of the molar conductivity of 1 mM DMSO solutions of the complexes (Λ_M) are in the range of 6–10 S cm^2 mol^{-1}. Thus, we may consider that **1–4** do not dissociate in DMSO solution, since for a 1 : 1 electrolyte, the Λ_M value should be ~70 S cm^2 mol^{-1}.

Compounds **1–4** are paramagnetic and show μ_{eff} values (= 1.78–1.98 BM) that are higher than the theoretically expected spin-only value (= 1.73 BM) at room temperature for a mononuclear Cu(II) complex with d^9 configuration (S = 1/2).[55] Similar μ_{eff} values were found for reported Cu(II)–quinolone derivatives.[26,37]

Stability of the complexes in solution

The UV-vis spectra of complexes **1–4** were recorded in DMSO solutions and as nujol mulls. In the solution spectra, there is a low-intensity band in the 685–735 nm region (ε = 30–125 M^{-1} cm^{-1}) which can be attributed to the d–d transitions; this band is typical for distorted square pyramidal geometry.[55] Further bands appearing in the UV region of the spectra are attributed to intraligand transitions, confirming the presence and the coordination of ligands. The UV-vis spectra of **1–4** in nujol are similar to those in DMSO solution, suggesting the preservation of the structure upon dissolution. The UV-vis spectra of **1–4** were also recorded in the presence of a series of buffer solutions with pH in the 6–8 range (150 mM NaCl and 15 mM trisodium citrate at pH values regulated by $HCl_{(aq)}$). These spectra show no significant change (*i.e.*, shift of λ_{max} of the existing bands or appearance of new bands), thus also confirming the integrity of the complexes in the buffer solutions used

for the biological experiments. The observed behavior of **1–4** is in good agreement with recent reports on related metal–quinolone derivatives.[26,37]

Structural features

X-ray crystal structures of 2–4

The crystal structures of complexes **2–4** are depicted in Fig. 2 and selected bond distances and angles are cited in Table S2 (ESI†). The structures are discussed together along with their similarities and differences. There are water solvate molecules in all three complexes and methanol solvate molecules in complexes **3** and **4**.

Compounds **2–4** are mononuclear and bear a deprotonated pefloxacin ligand that is bound to the Cu(1) atom in a bidentate chelating mode through the carboxylate O(1) and pyridone O(3) oxygen atoms, leading to the formation of a six-membered chelate ring. The N,N′-donor ligands bipyam, phen and bipy are coordinated bidentately to Cu(1) through the two aromatic nitrogen atoms N(1) and N(2) forming a six-membered (in **2**) and a five-membered (in **3** and **4**) chelate ring. In all three structures **2–4**, the Cu(1)–O distances [= 1.912(2)–1.9548(16) Å] are shorter than the Cu(1)–N distances [= 2.005(2)–2.023(2) Å], being comparable to those of related compounds.[26,37]

The five-coordinate Cu(1) atom presents a slightly distorted square pyramidal $\{CuN_2O_2Cl\}$ geometry as indicated by the values of tetragonality T^5 and trigonality index τ (Table S2, ESI†). The determination of T^5 is based on the changes in bond lengths,[56] while τ is calculated by the equation $\tau = (\varphi_1 - \varphi_2)/60^\circ$, where φ_1 and φ_2 are the largest angles in the coordination sphere. The τ values can vary from 0 to 1, with $\tau = 0$ corresponding to a perfect square pyramid and $\tau = 1$ to a perfect trigonal bipyramid.[57] The T^5 and τ values are 0.772 and 0.068 for **2**, 0.786 and 0.036 for **3**, and 0.776 and 0.041 for **4**, respectively, suggesting a slight distortion from the regular square-based pyramidal geometry as observed in related compounds.[25] For such an arrangement around the copper ion, the quinolone oxygen atoms O(1) and O(3) and the N,N′-donor nitrogen atoms N(1) and N(2) occupy the vertices of the basal plane, with the copper atom being displaced from the basal plane toward the Cl(1) atom which lies at the apical position of the pyramid.

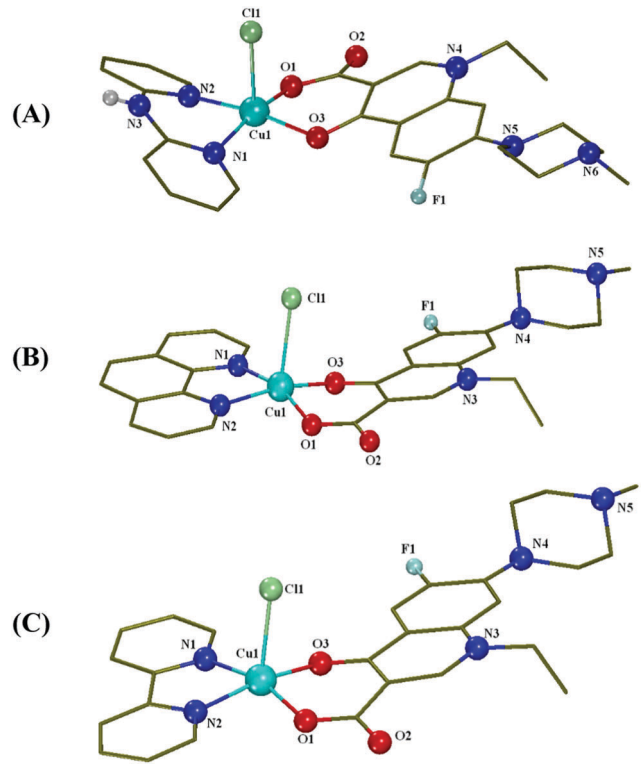

Fig. 2 Molecular structures of complexes (A) **2**, (B) **3** and (C) **4** with only the heteroatom labeling. Hydrogen atoms and solvate (methanol and water) molecules are omitted for clarity.

Proposed structure of 1

Our continuous attempts to grow crystals of complex **1** suitable for X-ray crystallography were not successful. Therefore, we may propose a structure for complex **1** on the basis of the experimental data (IR and UV-vis spectroscopy, elemental analysis, molar conductivity and magnetic measurements) and after a comparison with the reported structurally characterized Cu(II)–quinolone complexes. According to the magnetic data, the complex is mononuclear and the d–d band observed in the UV-vis spectra suggests a distorted square pyramidal geometry around the Cu(II) ion. On the basis of IR spectra, the deprotonated pefloxacin ligands are in a chelate bidentate binding manner through the pyridone and a carboxylato oxygen. Therefore, complex **1** is expected to have a structure similar to those of $[Cu(oflo)_2(H_2O)]$ (Hoflo = ofloxacin),[36] $[Zn(oflo)_2(H_2O)]$,[58] and $[Zn(pef)_2(H_2O)]$.[12]

Water and hybrid water–methanol clusters in structures of 2–4

An interesting feature of the obtained crystal structures consists of the H-bonding interactions of crystallization water and methanol molecules.[59] These are arranged into different types of solvent aggregates (Fig. S1, ESI†) which include a water dimer $(H_2O)_2$ in **2** and an infinite zigzag $(H_2O)_{5n}$ chain in **4**; this chain can be classified within the C4 type according to a classification of water clusters.[59a] In complexes **3** and **4**, there are also hybrid water–methanol associates $(H_2O)_2(MeOH)$ and $(H_2O)_3(MeOH)$, respectively; these can be classified within the D3 type.[59a] All these clusters are multiply H-bonded to the monocopper(II) molecular units, thus resulting in generation of 1D (**2**), 2D (**3**) or 3D (**4**) networks.

Topological description of H-bonded networks

To get further insight into the complex H-bonded nets, we simplified them by reducing the copper(II) complex units and solvent clusters into the corresponding centroids. Then, the obtained underlying nets were analyzed and classified from a topological perspective. An underlying 1D H-bonded chain in complex **2** (Fig. 3(A)) can be described as a uninodal 2-connected net with the decorated 2C1 topology. An underlying 2D H-bonded layer in compound **3** (Fig. 3(B)) is composed of the 3-connected

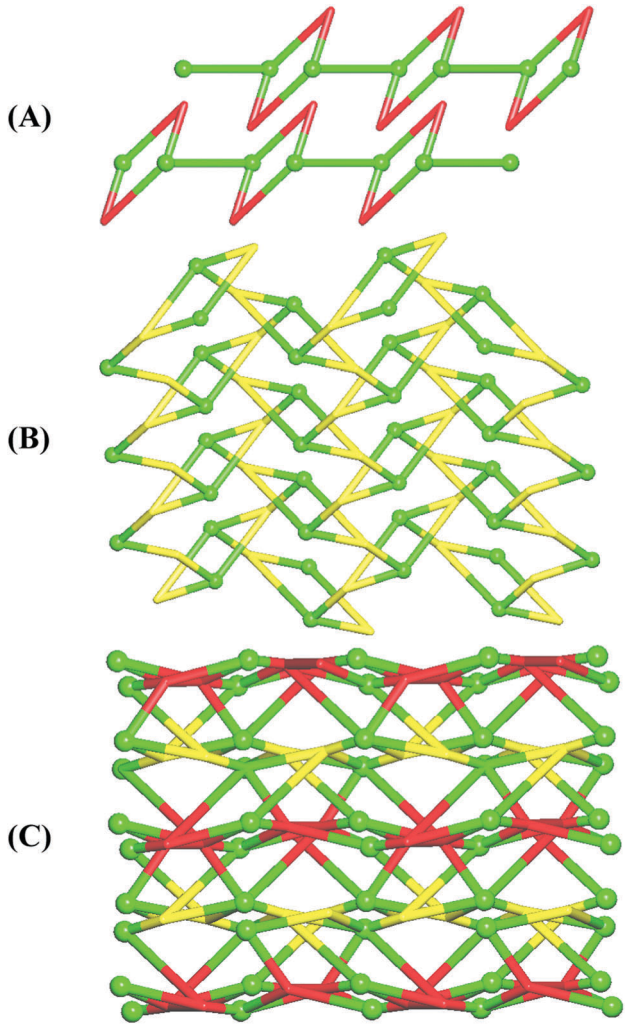

Fig. 3 Topological representation of the underlying H-bonded networks. (A) 1D chains in **2** showing a uninodal 2-connected net with the decorated 2C1 topology; view along the *a* axis; color codes: centroids of [Cu(pef)(bipyam)Cl] molecular nodes (green balls), centroids of $(H_2O)_2$ clusters (red). (B) 2D layer in **3** showing a uninodal 3-connected net with the fes [Shubnikov plane net $(4{\cdot}8^2)$] topology; view along the *a* axis; color codes: centroids of 3-connected [Cu(pef)(phen)Cl] molecular nodes (green balls), centroids of 3-connected $(H_2O)_2$(MeOH) cluster nodes (yellow). (C) 3D framework in complex **4** showing a tetranodal 4,4,5,7-connected net with a unique topology; view along the *c* axis; color codes: centroids of 4- and 5-connected [Cu(pef)(bipy)Cl] molecular nodes (green balls), centroids of 4-connected $(H_2O)_3$(MeOH) cluster nodes (yellow), centroids of 7-connected $(H_2O)_{5n}$ nodes (red).

[Cu(pef)(phen)Cl] molecular nodes and the 3-connected $(H_2O)_2$(MeOH) cluster nodes. These are topologically equivalent and give rise to a uninodal 3-connected net with the fes [Shubnikov plane net $(4{\cdot}8^2)$] topology and the point symbol $(4{\cdot}8^2)$. The 3D H-bonded framework of **4** is significantly more complex (Fig. 3(C)) due to the presence of the 4- and 5-connected [Cu(pef)(bipy)Cl] molecular nodes, 4-connected $(H_2O)_3$(MeOH) cluster nodes, and the 7-connected $(H_2O)_{5n}$ nodes. Topological analysis reveals a tetranodal 4,4,5,7-connected net with a unique topology and the point symbol $(3{\cdot}4^4{\cdot}5)(3^2{\cdot}4^3{\cdot}5^5{\cdot}6^5{\cdot}7^6)(4^2{\cdot}5^2{\cdot}7^2)(4^4{\cdot}5{\cdot}7^5)$.

Mild homogeneous catalytic oxidation of cycloalkanes

The copper(II) compounds **2–4** were tested as homogeneous catalysts for the oxidation of C_6–C_8 cycloalkanes to give a mixture of the corresponding cyclic alcohols and ketones. Cycloalkanes were selected as model substrates given the presence of only one type of aliphatic carbon atom in their structure as well as the practical importance of alkane oxidation reactions,[60–62] including the biological hydroxylation of alkanes by a copper containing enzyme, particulate methane monooxygenase.[63] The catalytic reactions were typically performed at 50 °C in air and in a MeCN/H_2O medium, using aqueous 50% H_2O_2 as an oxidant. As a solvent system, aqueous acetonitrile is widely considered as the best option in the mild homogeneous oxidation of alkanes by H_2O_2, especially given the stability of MeCN toward oxidation as well as the solubility of both alkane substrates and metal-complex catalysts.[53,54,60–62,64–68] The obtained results are presented in Fig. 4 and summarized in Table 1; all the product yields are based on the cycloalkane substrate.

The compounds **2–4** catalyze the oxidation of cycloalkanes and show a similar trend of substrate reactivity. Hence, for all the tested catalysts, the highest total yields of products were observed in the oxidation of cycloheptane (26–32%), followed by cyclooctane (20–29%) and cyclohexane (16–21%) (Table 1 and Fig. 4). In the oxidation of all cycloalkane substrates, the best activity is exhibited by **4** (Fig. 4(C)), while compounds **2** and **3** are slightly less efficient catalysts and show similar results. In all cases, cyclic alcohols are formed in slightly higher amounts than cyclic ketones (Table 1), and the typical alcohol/ketone molar ratios lie between 1.2 : 1 and 2.3 : 1.

The analysis of the kinetic curves in catalytic systems (Fig. 4) reveals that the oxidation reactions are rather quick; they are essentially complete within 40–60 min of the reaction time. The product yields do not increase appreciably on prolonging the reaction time up to 120 min. Besides, there is also no decline in the total product yields at a prolonged reaction time, thus suggesting that overoxidation of the products does not occur.

An important feature of the present catalytic systems concerns their ability to catalyze the oxidation of cycloalkanes without requiring any type of additive or co-catalyst. In fact, addition of trifluoroacetic acid as a recognized additive into the catalytic systems containing **2–4** does not lead to better product yields in comparison to those achieved in the absence of any additive (Table 1). This behavior significantly contrasts with the majority of Cu-based catalysts previously applied for the mild oxidation of cycloalkanes,[53,54,60–62,64–66] which usually need an acid promoter (strong mineral or carboxylic acid) to show an appreciable level of activity.

To evaluate the effects of various reaction parameters (amounts of catalyst, oxidant, substrate, and reaction temperature) on the catalytic activity of the present systems, we selected catalyst **4** and cycloheptane as a model system given the highest product yield achieved among the tested catalysts and substrates (Table 1).

The effect of the catalyst amount on the total yield of the products and the maximum initial reaction rate (W_0) in the cycloheptane oxidation catalyzed by **4** is shown in Fig. 5. Both the total yield of cycloheptanol and cycloheptanone and

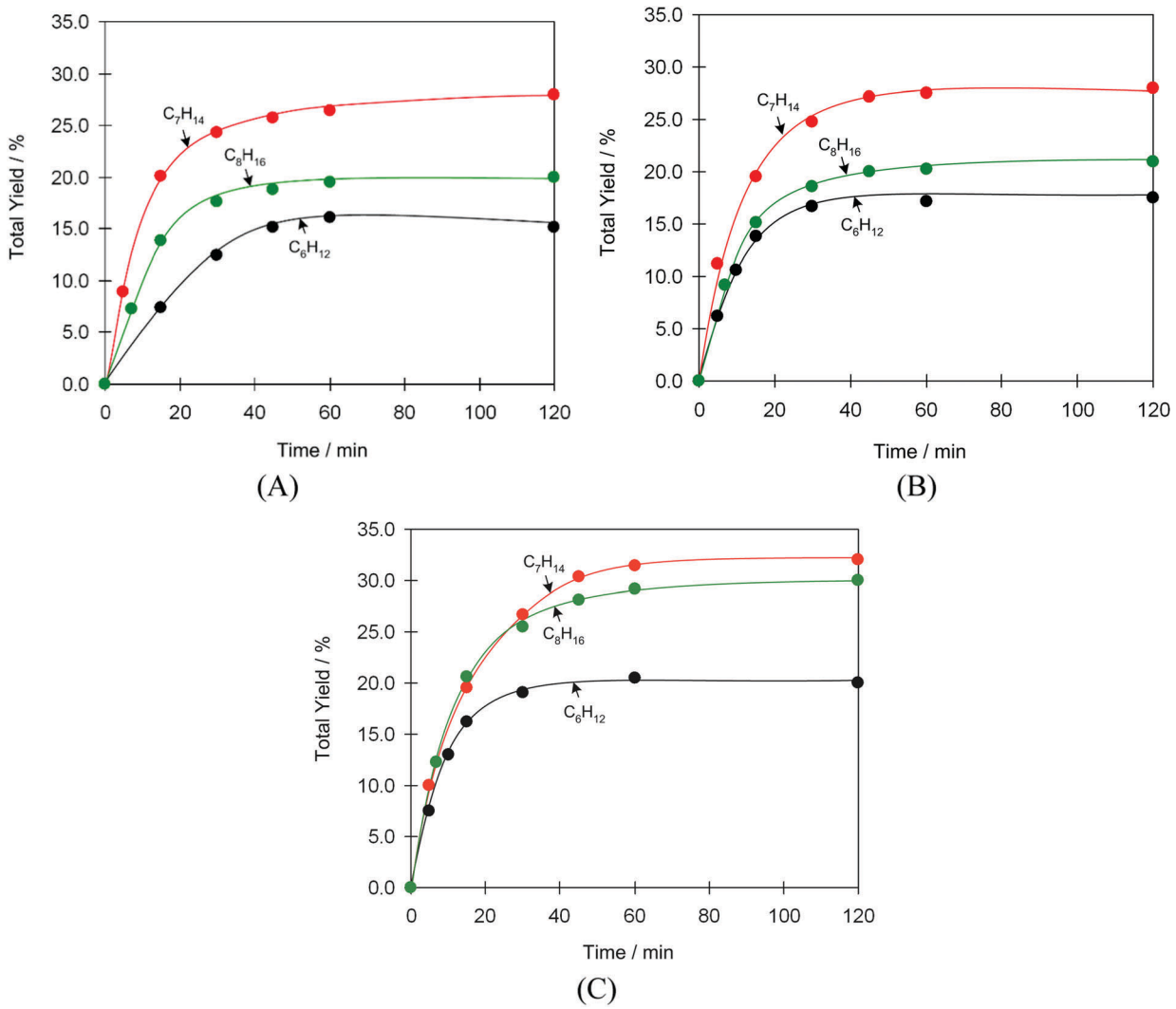

Fig. 4 Oxidation of cyclohexane, cycloheptane, and cyclooctane (total yield of the products *vs* time) with H_2O_2 catalyzed by complex (A) **2**, (B) **3** and (C) **4**. Reaction conditions: catalyst (5 μmol), cycloalkane (1.0 mmol), H_2O_2 (5.0 mmol), CH_3CN (up to total volume of 2.5 mL), 50 °C, 2 h.

the initial reaction rate gradually increase on raising the catalyst amount from 0.5 to 2.0 mM. Such a trend indicates first order dependence of W_0 on the concentration of **4**, thus indicating involvement of one type of the Cu-containing species in the rate-limiting catalytic step of the cycloheptane oxidation.

The oxidant amount also has an important effect on the product yield. An increase of the H_2O_2 concentration from 0.4 to 2.0 M leads to growth of the maximum total yield from 8 to 32% (Fig. 6). At the same time, at lower peroxide concentrations the oxidation reactions end very quickly (in ~10 min), thus preventing further yield growth. In contrast, at a higher H_2O_2 concentration (2 M) the maximum total yield of 32% is attained in ~60 min.

The total product yield (in mmol, Fig. 7(A)) increases on changing the cycloheptane concentration from 0.2 to 0.4 M, whereas further increase of the C_7H_{14} loading (up to 0.6 M) practically does not affect the reaction kinetics. The dependence of the initial reaction rate on the cycloheptane concentration (Fig. 7(C)) is close to linear in the low range of concentrations (up to 0.4 M C_7H_{14}); after that, W_0 reaches a plateau and does not depend on the concentration of C_7H_{14}. Such a type of W_0 dependence on the substrate concentration is typical for the catalytic systems that operate with $HO^{\bullet}$ radicals.[53,54,61] The total product yield, in % based on the substrate, is higher at a low substrate loading (35% yield at 0.2 M C_7H_{14}) due to increased concentrations of other reagents relative to the substrate (Fig. 7(B)). Besides, the reaction system is restricted by a limited solubility of C_7H_{14} in the CH_3CN/H_2O reaction medium.

Reaction temperature is also an important parameter in the mild oxidation of cycloalkanes. Prior studies showed that gentle heating of the reaction mixture (from ambient temperature up to 50 °C) accelerates the alkane oxidation reactions, without providing a notable contribution to overoxidation of products, and decomposition of catalyst or oxidant.[61,64–67] This is in agreement with the present **4**/C_7H_{14} system, wherein the oxidation of cycloheptane proceeds much faster at 50 °C in

Table 1 Mild oxidation of C_6–C_8 cycloalkanes catalyzed by compounds **2–4**[a]

Substrate	Product yield[b], %		
	Alcohol	Ketone	Total[c]
Catalyst **2**			
Cyclohexane	9.5	6.6	16.1
Cycloheptane	14.9	11.5	26.4
Cyclooctane	11.0	8.5	19.5
Catalyst **3**			
Cyclohexane	11.9	5.2	17.1
Cycloheptane	17.0	10.5	27.5
Cyclooctane	11.0	9.2	20.2
Catalyst **4**			
Cyclohexane	14.8	5.7	20.5
Cycloheptane	18.5	13.2	31.7
Cyclooctane	16.9	12.3	29.2

[a] Reaction conditions: cycloalkane (1 mmol), catalyst (5 μmol), H_2O_2 (50% aq., 5 mmol), MeCN (up to 2.5 mL total volume), 50 °C, 2 h. [b] Yields are based on the cycloalkane substrate: (moles of product per mol of cycloalkane) × 100%. [c] Sum of the yields of alcohol and ketone products.

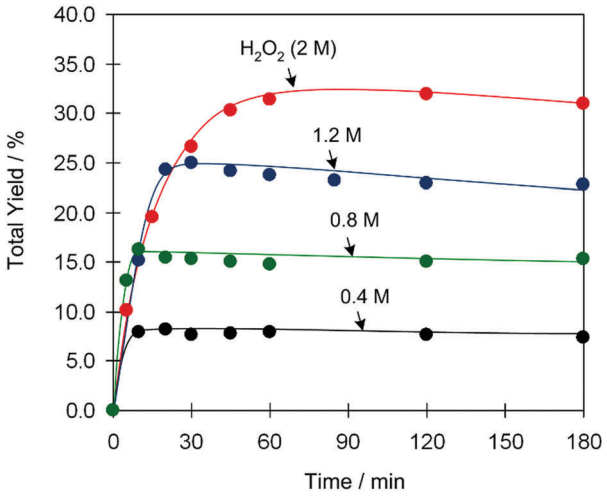

Fig. 6 Effect of the oxidant amount on the total yield of the products (cycloheptanol and cycloheptanone) in the cycloheptane oxidation catalyzed by **4**. Reaction conditions: catalyst **4** (5.0 μmol), C_7H_{14} (1.0 mmol), H_2O_2 (0.4–2 M), CH_3CN (up to 2.5 mL total volume), 50 °C.

comparison with the reaction at 30 °C (Fig. 8). Besides, the maximum total yield of 32% can be achieved in 60 min at 50 °C, whereas the reaction at 30 °C requires a much longer reaction time to attain a comparable yield (25% in 300 min).

To get some information on the nature of the oxidizing species and on the selectivity parameters in the present reactions, we investigated the mild oxidation of *n*-heptane and methylcyclohexane as model substrates (Table 2). For all the catalysts, the oxidation of *n*-C_7H_{16} proceeds without a specific preference for any secondary C atom of the *n*-heptane chain and leads to indiscriminative regioselectivity parameters C(1) : C(2) : C(3) : C(4) of 1 : 6 : 6 : 6, 1 : 5 : 5 : 5, or 1 : 4 : 4 : 6 for **2**, **3**, or **4**, respectively. In the oxidation of methylcyclohexane, the bond selectivity parameters 1° : 2° : 3° of 1 : 5 : 10 (**2**), 1 : 5 : 7 (**3**), or 1 : 4 : 8 (**4**) are also rather similar and indicate that the tertiary C atom is oxidized with some preference over the secondary carbon atoms. Such regioselectivity and bond selectivity parameters are comparable to those reported for other copper-complex catalysts, suggesting free radical mechanisms and an involvement of hydroxyl radicals as a powerful and rather indiscriminate oxidizing species.[64–67] Thus, the HO• radicals abstract the H atoms from an alkane (RH) to generate alkyl radicals (R•). These then react with O_2 (*e.g.*, from air or formed from H_2O_2) to form alkyl peroxy radicals (ROO•). The latter then

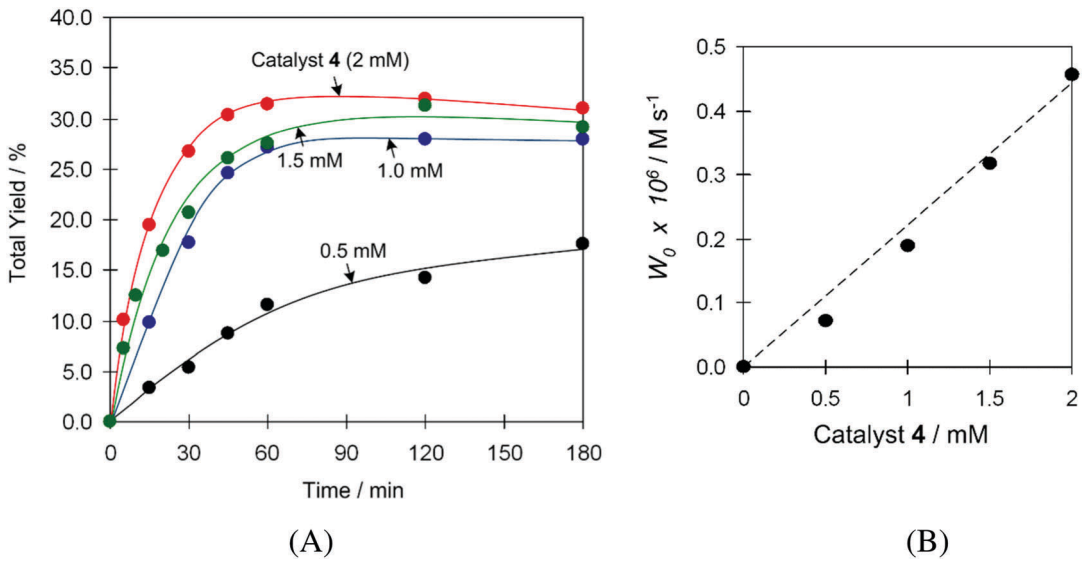

Fig. 5 Effect of the catalyst amount on (A) the total yield of the products (cycloheptanol and cycloheptanone) and (B) initial reaction rate (W_0) in the cycloheptane oxidation catalyzed by **4**. Reaction conditions: catalyst **4** (5 μmol), C_7H_{14} (1.0 mmol), H_2O_2 (5.0 mmol), CH_3CN (up to 2.5 mL total volume), 50 °C.

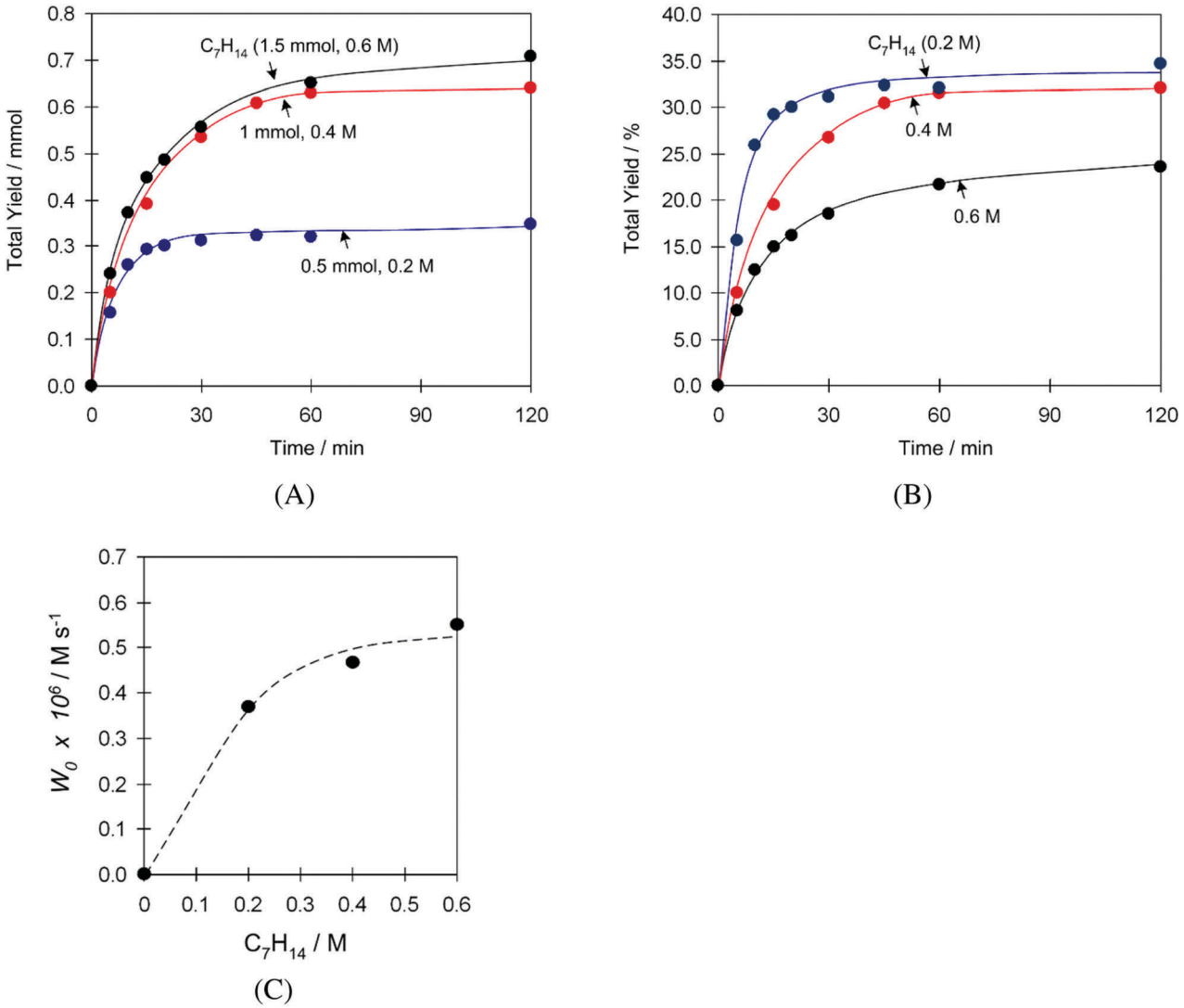

Fig. 7 Effect of the substrate (C_7H_{14}) amount on (A and B) the total yield (in mmol and %) of the products and (C) the initial reaction rate (W_0) in the cycloheptane oxidation catalyzed by **4**. Reaction conditions: catalyst **4** (5 μmol), C_7H_{14} (0.5–1.5 mmol; 0.2–0.6 M), H_2O_2 (5.0 mmol), CH_3CN (up to 2.5 mL total volume), 50 °C.

give alkyl hydroperoxides (ROOH) as primary intermediate products; their formation was confirmed by GC analysis following a method developed by Shul'pin.[53,54] Alkyl hydroperoxides quickly decompose to the corresponding alcohols and ketones as final oxidation products.[64–67]

Biological activity studies

We also performed standard biological experiments with isolated copper(II) pefloxacin complexes. Such studies include evaluation of the antimicrobial activity of the compounds and their interaction with serum proteins (HSA, BSA) and CTA DNA. This enables us to compare the results with our previous data on other copper(II) quinolone complexes. The bioactivity tests were performed under standard conditions, without addition of reducing agents or hydrogen peroxide. Herein only the most important results are briefly reported and the corresponding figures are given in the ESI.†

Antimicrobial activity

The antimicrobial potential of pefloxacin and its copper(II) derivatives **1–4** was evaluated against two Gram-positive (*B. subtilis, S. aureus*) and two Gram-negative (*X. campestris, E. coli*) bacteria (Table 3). Hpef and complexes **1–4** are highly active against all four bacteria tested and exhibit MIC values in the range of 0.25–2.0 μg mL^{-1} (0.33–3.41 μM). Compounds **1–4** are thus among the most active antimicrobials if compared with other examples of Cu(II)-quinolone derivatives [Cu(Q)(N,N-donor)Cl].[25,28,33,37,38,69–71] In particular, complex **1** (the only compound without a N,N′-donor) is as active as Hpef against the microorganisms tested and more active than complexes **2–4** against the Gram-(−) bacteria. In addition, when the MIC values expressed in μM are considered, complexes **2–4** are equally active to Hpef, while **1** is an even more potent antimicrobial than pefloxacin. There are five commonly accepted

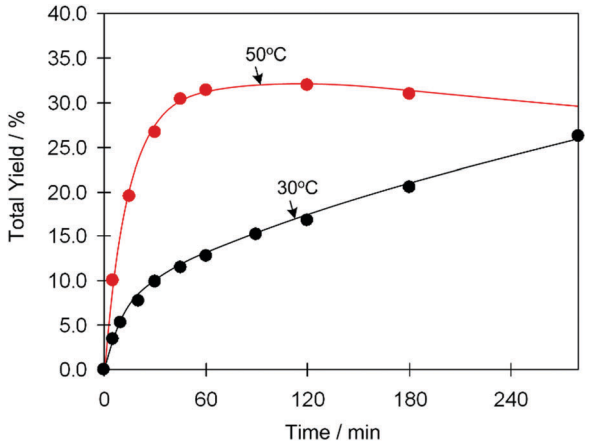

Fig. 8 Effect of the reaction temperature on the total yield of the products (cycloheptanol and cycloheptanone) in the cycloheptane oxidation catalyzed by **4**. Reaction conditions: catalyst **4** (5.0 μmol), C_7H_{14} (1.0 mmol), H_2O_2 (5.0 mmol), CH_3CN (up to 2.5 mL total volume), 30 or 50 °C.

Table 2 Selectivity parameters in the oxidation of *n*-heptane and methylcyclohexane[a]

Selectivity parameter	2	3	4
Regioselectivity C(1):C(2):C(3):C(4)[b] (*n*-C_7H_{16})	1:6:6:6	1:5:5:5	1:4:4:6
Bond selectivity 1°:2°:3° (methylcyclohexane)[c]	1:5:10	1:5:7	1:4:8

[a] Reaction conditions: catalyst (5 μmol), alkane (1.0 mmol), H_2O_2 (5.0 mmol), MeCN up to 2.5 mL total volume, 2 h, 50 °C. All parameters were calculated based on the ratios of isomeric alcohols. The calculated parameters were normalized, *i.e.* recalculated taking into account the number of H atoms at each carbon atom. [b] Parameters C(1):C(2):C(3):C(4) are the relative reactivities of hydrogen atoms at carbons 1, 2, 3, and 4 of the *n*-heptane chain. [c] Parameters 1°:2°:3° are the relative normalized reactivities of the hydrogen atoms at primary, secondary, and tertiary carbon atoms of methylcyclohexane.

Table 3 Antimicrobial activity of Hpef and complexes **1–4** expressed in MIC in μg mL^{-1} or μM (the values in parentheses)

Compound	*E. coli*	*X. campestris*	*S. aureus*	*B. subtilis*
Pefloxacin (Hpef)	0.5 (1.50)	0.5 (1.50)	0.25 (0.75)	0.5 (1.50)
$[Cu(pef)_2(MeOH)]$, **1**	0.5 (0.66)	0.5 (0.66)	0.25 (0.33)	1 (1.32)
[Cu(pef)(bipyam)Cl], **2**	1 (1.66)	1 (1.66)	0.5 (0.83)	1 (1.66)
[Cu(pef)(phen)Cl], **3**	1 (1.64)	1 (1.64)	0.5 (0.82)	1 (1.64)
[Cu(pef)(bipy)Cl], **4**	1 (1.70)	1 (1.70)	0.5 (0.85)	2 (3.41)

factors that influence the antimicrobial activity of the complexes,[72,73] namely: (i) the chelate effect of ligands, (ii) the nature of ligands, (iii) the nuclearity, (iv) the total charge, and (v) the presence and the nature of counterions. Among these factors, we may suggest that the coordination of pefloxacin to Cu(II) which results in the formation of the chelate ring is the most important one for the enhanced antimicrobial activity of **1–4** if compared to Hpef. Further, the antimicrobial activity of the complexes seems to be dependent on the number of pef ligands in the complex.

Interaction of the compounds with serum albumins

The study of the interaction of bioactive compounds with serum albumins (SAs), proteins that participate in the transportation of ions and drugs toward cells and tissues,[74] is a first approach to explain the potential biological activity, since their binding to SAs may influence the biological properties or may reveal novel alternative transportation pathways or mechanisms.[75] The quenching of the SA-fluorescence emission band in the presence of copper(II) compounds is much more pronounced for BSA, with the maximum quenching observed in the presence of **2** (up to 51.0% and 78.0% for HSA and BSA, respectively, Fig. S2 and S3, ESI†). This quenching may be attributed to possible changes in the tryptophan environment of SA, probably due to changes in the albumin secondary structure.[75]

The SA-quenching constants (k_q) of the compounds were calculated from the corresponding Stern–Volmer plots (Fig. S4 and S5, ESI†) and the Stern–Volmer quenching equation (eqn (S2) and (S3)). These constants are much higher (Table 4) than the value of 10^{10} M^{-1} s^{-1} and suggest the existence of a static quenching mechanism[76] with the binding of the compounds to SA.[77] The k_q constants of the complexes are higher than the corresponding values for free Hpef. Complexes **1** and **2** feature the highest k_q constants for HSA and BSA, respectively. On average, the k_q constants are within the range (10^{12}–10^{13} M^{-1} s^{-1}) found for a series of metal-complexes bearing quinolones as ligands.[25,26,37,69]

The SA-binding constants (K), calculated from the Scatchard plots (Fig. S6 and S7, ESI†) and the Scatchard equation (eqn (S4)), are moderate-to-high (Table 4) and are of the same magnitude as those reported for other metal–quinolone complexes.[25,26,37,69] Complexes **1–4** bind tighter to BSA than to HSA. Compound **2** has the highest K constant for BSA, whereas complexes **2** and **3** display the highest K constants for HSA among the present compounds. The K constants are in the 1.56×10^4–8.65×10^5 M^{-1} range, being indicative of the SA-binding and migration of the compounds to the sites of potential biological targets. On the other hand, a comparison of these constants with the K value of the strongest non-covalent interaction, *i.e.* $K \sim 10^{15}$ M^{-1} regarding the interaction of avidin with diverse compounds,[78] may reveal a reversibility of the binding of the compounds to the SAs which is essential for their potential release upon arrival at biotargets.

Table 4 The albumin constants for Hpef and complexes **1–4**

Compound	$k_{q(BSA)}$ (M^{-1} s^{-1})	$k_{q(HSA)}$ (M^{-1} s^{-1})	$K_{(BSA)}$ (M^{-1})	$K_{(HSA)}$ (M^{-1})
Hpef	$8.46(\pm0.10) \times 10^{11}$	$1.15(\pm0.12) \times 10^{12}$	$2.51(\pm0.12) \times 10^5$	$5.13(\pm0.35) \times 10^5$
$[Cu(pef)_2(MeOH)]$, **1**	$1.69(\pm0.05) \times 10^{13}$	$2.64(\pm0.15) \times 10^{12}$	$1.77(\pm0.06) \times 10^5$	$1.56(\pm0.43) \times 10^4$
[Cu(pef)(bipyam)Cl], **2**	$1.26(\pm0.07) \times 10^{13}$	$6.05(\pm0.40) \times 10^{12}$	$8.65(\pm0.37) \times 10^5$	$1.23(\pm0.10) \times 10^5$
[Cu(pef)(phen)Cl], **3**	$1.04(\pm0.05) \times 10^{13}$	$5.46(\pm0.25) \times 10^{12}$	$9.50(\pm0.10) \times 10^4$	$1.24(\pm0.06) \times 10^5$
[Cu(pef)(bipy)Cl], **4**	$5.52(\pm0.26) \times 10^{12}$	$1.53(\pm0.11) \times 10^{12}$	$1.14(\pm0.08) \times 10^5$	$4.78(\pm0.40) \times 10^4$

Interaction of the compounds with CT DNA

The interaction of metal complexes with CT DNA, and especially the ones bearing quinolones as ligands, is of increasing research interest due to the biological role of quinolones in targeting the enzymes DNA gyrase and topoisomerase IV, which are responsible for DNA-replication.[1,2,9] In general, the interaction of metal complexes may take place covalently or noncovalently (including intercalation, groove-binding or electrostatic interactions) and depends mainly on the stability and the nature of the complexes.[79,80]

The changes observed in the UV spectra of CT DNA solution in the presence of Hpef and **1–4** (Fig. S8, ESI†), as well as in the spectra of similar solutions having increasing amounts of CT DNA (Fig. S9, ESI†), indicate the interaction of the studied compounds with CT DNA.[81] The percentage of hypochromism in most cases is not sufficiently intense (Table 5) to conclude unambiguously the DNA-interaction mode of the complexes.

The DNA-binding constants (K_b) of complexes **1–4**, as calculated by the Wolfe–Shimer equation (eqn (S5))[82] and the respective plots (Fig. S10, ESI†), are higher than that of Hpef suggesting their tighter binding to CT DNA upon coordination to Cu. The highest K_b constant among the compounds is observed for complex **2** (Table 5), which is among the tightest DNA-binders reported for metal–quinolone complexes.[25,26,37,69]

The DNA-viscosity changes (η/η_0) depend on the relative DNA-length changes (L/L_0) in the presence of a DNA-binder and are related by the equation $L/L_0 = (\eta/\eta_0)^{1/3}$.[83] Therefore, the DNA-binding mode of the compounds may be clarified by monitoring the DNA-viscosity changes in the presence of the compounds. The viscosity changes of a DNA solution (0.1 mM) were monitored in the presence of increasing amounts of the compounds (up to the value of $r = 0.35$). Upon addition of the compounds, a significant increase of the relative DNA-viscosity is observed (Fig. 9), indicating that the interaction of the compounds with DNA takes place probably *via* intercalation.[26,37,69,83]

EB is a typical intercalation marker since its intercalation in-between adjacent base pairs on the double DNA-helix *via* its planar EB phenanthridine ring results in the formation of the EB–DNA conjugate which presents an intense fluorescence emission band at 592 nm, when excited at 540 nm.[74,84] The fluorescence emission spectra of pre-treated EB–DNA conjugate ([EB] = 20 μM, [DNA] = 26 μM) were recorded for increasing amounts of the compounds and are representatively shown for complex **1** in Fig. S11(A) (ESI†). The addition of each compound resulted in significant quenching of the EB–DNA emission band at 592 nm (up to 79.5% of the initial EB fluorescence for complex **1**, Fig. S11(B) and Table 6, ESI†).

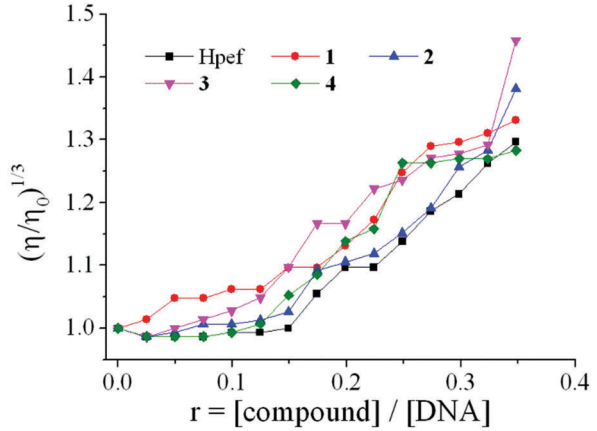

Fig. 9 Relative viscosity $(\eta/\eta_0)^{1/3}$ of CT DNA ([DNA] = 0.1 mM) in buffer solution (150 mM NaCl and 15 mM trisodium citrate at pH 7.0) in the presence of Hpef and complexes **1–4** in increasing amounts (r = [complex]/[DNA]).

This quenching is in good agreement ($R \sim 0.99$, Fig. S12, ESI†) with the linear Stern–Volmer equation (eqn (S2)) and may be assigned to the displacement of EB from the EB–DNA conjugate by the compounds, as a possible result of their competition with EB for the intercalation DNA-sites. The K_{SV} constants (Table 6) are in the range reported for other metal–quinolones,[26,37,69] with complex **1** having the highest K_{SV} constant among the pefloxacin derivatives. The quenching constants (k_q) for the compounds (Table 6) are significantly higher than 10^{10} M^{-1} s^{-1}, suggesting a static mechanism for the quenching of the EB−DNA fluorescence; they also prove the EB-displacement and the simultaneous binding of the compounds under study. Therefore, the intercalation of the compounds to DNA may be indirectly verified.[76]

Interaction of copper(II)–quinolone complexes with biomolecules

Considering the reported copper(II)–quinolone complexes, we may compare the biological behavior (antimicrobial activity and binding with DNA and albumins) of the present pefloxacin compounds **1–4** with their copper(II) analogues bearing the quinolones enrofloxacin (Herx),[33] flumequine (Hflmq),[26,69] gatifloxacin (Hgati),[27] norfloxacin (Hnorf),[34] ofloxacin (Hoflo),[34] oxolinic acid (Hoxo),[28] pipemidic acid (HPPA),[85] *N*-propyl-norfloxacin (Hpr-norf)[85] and sparfloxacin (Hsf)[70] as ligands (Tables S4 and S5, ESI†). It should

Table 5 Spectral features of the interaction of Hpef and its copper(II) complexes **1–4** upon addition of DNA. UV-band (λ_{max}, in nm) (percentage of the observed hyper-/hypo-chromism ($\Delta A/A_0$, %), blue-/red-shift of λ_{max} ($\Delta\lambda$, nm)) and the corresponding DNA-binding constants (K_b)

Compound	Band ($\Delta A/A_0$[a], $\Delta\lambda$[b])	K_b (M^{-1})
pefloxacin	285 (+3.5, −4); 318 (−2, +1)	$6.05(\pm0.12) \times 10^4$
[Cu(pef)$_2$(MeOH)], **1**	286 (−6, −2); 320 (−4.5, +3)	$4.99(\pm0.14) \times 10^5$
[Cu(pef)(bipyam)Cl], **2**	319 (−5, −3)	$8.46(\pm0.05) \times 10^6$
[Cu(pef)(phen)Cl], **3**	291 (−4.3, 0); 326 (−16, +3)	$7.83(\pm0.35) \times 10^4$
[Cu(pef)(bipy)Cl], **4**	291 (−4.5, −2); 313(sh) (−30, elm[c]); 333 (−21, +5)	$6.86(\pm0.20) \times 10^5$

[a] "+" denotes hyperchromism, "−" denotes hypochromism. [b] "+" denotes red-shift, "−" denotes blue-shift. [c] "elm" = eliminates.

Table 6 Percentage of EB–DNA fluorescence quenching ($\Delta I/I_o$, %) and the Stern–Volmer (K_{SV} in M^{-1}) and EB–DNA quenching constants (k_q, $M^{-1}\,s^{-1}$) for pefloxacin and its complexes **1–4**

Compound	$\Delta I/I_o$ (%)	K_{sv} (M^{-1})	k_q ($M^{-1}\,s^{-1}$)
Hpef	70.8	$7.00(\pm0.36) \times 10^4$	$3.04(\pm0.16) \times 10^{12}$
[Cu(pef)$_2$(MeOH)], **1**	79.5	$9.91(\pm0.26) \times 10^5$	$4.31(\pm0.12) \times 10^{13}$
[Cu(pef)(bipyam)Cl], **2**	74.3	$2.37(\pm0.07) \times 10^5$	$1.03(\pm0.03) \times 10^{13}$
[Cu(pef)(phen)Cl], **3**	74.6	$2.53(\pm0.04) \times 10^5$	$1.10(\pm0.02) \times 10^{13}$
[Cu(pef)(bipy)Cl], **4**	74.7	$1.67(\pm0.05) \times 10^5$	$7.26(\pm0.20) \times 10^{12}$

be noted that Hflmq, Hoxo and HPPA are first-generation quinolones, Herx, Hnorf, Hoflo and Hpr-norf are second-generation quinolones (similar to Hpef), and Hgati and Hsf are third-generation quinolones.

As seen in Table S4 (ESI†), the antimicrobial activities of the copper–quinolone complexes are similar or slightly better than those of the corresponding free quinolones. The main factor affecting the range of the antimicrobial activity of these complexes is the generation of the quinolone ligand; the higher the generation of the quinolone, the more active the compound. A general conclusion of whether the presence of an N,N′-donor ligand enhances the biological activity cannot be drawn, since its presence may ameliorate the activity (as for Cu(II)–gatifloxacin complexes) and may not induce significant variances.[25]

In regard to the DNA-binding constants (Table S5, ESI†), the generation of the quinolone does not seem to affect the magnitude of K_b. On the other hand, the presence of the N,N′-donor ligand seems, on average, to enhance the affinity of the compounds to DNA. The conclusions regarding the binding affinity for the albumins are quite similar in general (Table S5, ESI†), *i.e.* copper(II)–quinolone complexes with the CuN_2O_2Cl coordination sphere have higher SA-binding constants than the complexes with the CuO_5 environment.

We would also like to mention some previous biological studies which might be important for better understanding of catalytic results in the present work. For example, DNA cleavage activity of various copper ciprofloxacin (cfH) complexes was also tested.[32] It was observed that after 4 h incubation in the presence of a reducing agent ascorbate, a ternary complex [CuCl(cfH)(phen)]Cl·2H_2O completely fragmented DNA. Apart from this complex, the measurable nuclease activity was only observed with the mixed-valence Cu(II)/Cu(I) compound [$Cu^{II}(cfH)_2(Cu^{I}Cl_2)_2$] but not with the copper(II) complex containing only quinolone ciprofloxacin ([Cu(cfH)$_2$Cl$_2$]·6H_2O). In an additional experiment, H_2O_2 was added and after that all the studied compounds exert measurable nuclease activity. Interesting results were recently obtained also by Kyziol *et al.* who studied the biological properties of Cu(II) and Cu(I) complexes of various quinolone derivatives.[86] They have found that Cu(I) complexes were much more active but Cu(II) complexes were more efficient in producing reactive oxygen species. Obviously, the oxidation state of the metal and conditions used in experiments (*e.g.*, use of reducing agent, hydrogen peroxide) are very important in such systems. Various reactive oxygen species are formed in all aerobic organisms but the levels are low and are regulated. For example, the physiological range for the intracellular H_2O_2 concentration is relatively uniform in aerobic forms of life, and appears to vary from ~0.001 μM to 0.7 μM. Low endogenous levels of H_2O_2 are maintained by the catalase enzyme that catalyzes its decomposition to water and oxygen.[87] Although the conditions used in our catalytic experiments are clearly very different from those used in the above described biological experiments (higher concentration of H_2O_2, higher temperature, different solvent), there are some observations which are valid for both types of results. It seems that our complexes containing Cu(II) ions and quinolone but no N,N′-donor ligand are not good catalysts and can also not substantially cleave DNA without addition of hydrogen peroxide. It also seems probable that formation of reactive oxygen species is important for both types of activities. Without any doubt, further studies would be needed to claim that such copper complexes can catalyze important reactions in living systems. However, it could also not be totally excluded that various types of copper (or other metal) complexes are formed in the human body and that some might be involved in processes that are important for side effects of quinolone drugs.

Conclusions

In the present work, we described the synthesis and characterization of mononuclear copper compounds with a second-generation quinolone antibacterial drug (pefloxacin) in the absence or presence of nitrogen-donor heterocyclic ligands such as bipyam, phen or bipy. In the resultant copper(II) complexes, the quinolone ligands are deprotonated and coordinated to copper in a bidentate chelating mode through the pyridone and a carboxylato oxygen. The crystal structures of [Cu(pef)(bipyam)Cl], [Cu(pef)(phen)Cl] and [Cu(pef)(bipy)Cl] were determined by X-ray crystallography, revealing a distorted square–pyramidal geometry for Cu(II) and presenting a similar arrangement of the atoms around copper.

We also showed that the discrete monocopper(II) complexes are extended into diverse 1D, 2D, or 3D H-bonded networks *via* multiple hydrogen bonding interactions with crystallization solvent molecules. In turn, water and/or methanol molecules of crystallization are arranged into different types of H-bonded clusters, including hybrid water–methanol associates and infinite 1D water tapes. Topological analysis and classification of the simplified H-bonded nets was performed. Hence, the present study also contributes to the detection of different water assemblies trapped by various metal–organic materials as well as to topological classification of complex H-bonded nets.

Besides, we have also disclosed an application of the obtained copper(II) compounds as efficient homogeneous catalysts for the mild oxidation of cycloalkanes to give a mixture of cyclic alcohols and ketones. These reactions proceed rather quickly and under mild conditions (50 °C, atmospheric pressure), in the absence of any additional promoter or co-catalyst, and lead to maximum product yields up to 35% based on a cycloalkane substrate. Such a level of product yields is rather high in the field of mild alkane oxidation, especially if the high inertness of these hydrocarbons

and mild reaction conditions are considered. In fact, an industrial process (DuPont) for the oxidation of cyclohexane uses a homogeneous cobalt naphthenate catalyst and proceeds with only ~5% cyclohexane conversion under harsher reaction conditions.[88] Interestingly, complex **1** appeared to be inactive in the present type of cycloalkane oxidations, which is most likely associated with its fast decomposition in the reaction medium. In comparison with **2–4**, such a behavior of **1** can be related to the absence of chloride and N,N′-donor aromatic ligands in its structure. Furthermore, the effects of different reaction parameters on the catalytic activity of catalyst **4** in the oxidation of cycloheptane (a model system) were investigated. We believe that the present work might open up a novel application of the Cu–quinolone coordination compounds in catalysis. Further research on the application of such copper(II) catalysts in the oxidative functionalization of alkanes and on widening the substrate scope of such reactions will be pursued.

All the obtained compounds also showed significant antimicrobial activity, with MIC values ranging from 0.25 to 2.0 μg mL^{-1} (0.33–3.64 μM). Such a level of activity in most cases is enhanced in comparison to free pefloxacin. The interaction of the complexes with albumins showed that they exhibit high affinity for albumins and especially for BSA. All the SA-binding constants of the compounds are of the order 10^4–10^5 M^{-1}, proving their ability to bind reversibly to the albumins in order to get transferred toward their potential biological targets. The copper(II)–pefloxacin complexes can bind to CT DNA in an intercalative mode as revealed by the techniques employed in the present study. The complexes exhibit higher binding constants to CT DNA than free pefloxacin, with complex **2** having the highest calculated K_b constant among the present compounds, which also lies among the highest K_b values reported for metal–quinolone complexes.

In conclusion, the present work extended a still very limited family of structurally characterized pefloxacin coordination compounds to their copper(II) examples. Apart from the structural significance of **1–4**, the Cu(II)–pefloxacin derivatives **2–4** exhibit notable catalytic activity. Besides, all the obtained compounds feature a very promising biological profile in regard to their interaction with biomacromolecules and their antibacterial activity, which deserve further attention and investigation. These studies will be pursued in our laboratories.

Abbreviations

B. subtilis	*Bacillus subtilis* ATCC 6633
bipy	2,2′-Bipyridine
bipyam	2,2′-bipyridylamine
BSA	bovine serum albumin
cfH	Ciprofloxacin
CT	Calf-thymus
E. coli	*Escherichia coli* NCTC 29212
EB	Ethidium bromide, 3,8-diamino-5-ethyl-6-phenyl-phenanthridinium bromide
Hpef	Pefloxacin, 1-ethyl-6-fluoro-7-(4-methylpiperazin-1-yl)-4-oxo-quinoline-3-carboxylic acid
HSA	Human serum albumin
K	SA-binding constant
K_b	DNA-binding constant
k_q	SA-quenching constant
K_{SV}	Stern–Volmer constant
m	Medium
MIC	Minimum inhibitory concentration
pef	Anion of pefloxacin
phen	1,10-Phenanthroline
r	[compound]/[DNA] ratio
r′	[DNA]/[compound] ratio
s	Strong
S. aureus	*Staphylococcus aureus* ATCC 6538;
SA	Serum albumin
sh	Shoulder
vs	very strong
X. campestris	*Xanthomonas campestris* ATCC 1395
$\Delta\nu(CO_2)$	$\nu_{asym}(CO_2) - \nu_{sym}(CO_2)$.

Conflicts of interest

There are no conflicts to declare.

Acknowledgements

This work has been supported by the FCT and Portugal 2020 (LISBOA-01-0145-FEDER-029697, IF/01395/2013/CP1163/CT005, CEECIND/03708/2017, UID/QUI/00100/2013). We would like to acknowledge networking support by the COST action CA15106 (CHAOS). The publication has also been prepared with the support of the RUDN University Program 5-100. Financial support from the Slovenian Research Agency (ARRS) through project P1-0175 and infrastructure (use of SuperNova diffractometer) of the EN–FIST, Center of Excellence, Trg OF 13, Ljubljana, Slovenia is gratefully acknowledged.

References

1 D. C. Hooper and E. Rubinstein, *Quinolone Antimicrobial Agents*, ASM Press, Washington, DC, USA, 3rd edn, 2003.
2 *The Quinolones*, ed. V. T. Andriole, Academic Press, 2000.
3 R. Huang, B. Wen, Z. Pei, X. Shan, S. Zhang and P. N. Williams, *Environ. Sci. Technol.*, 2009, **43**, 3688–3693.
4 J. Marchant, *Nature*, 2018, **555**, 431–433.
5 A. Wohlkonig, P. F. Chan, A. P. Fosberry, P. Homes, J. Z. Huang, M. Kranz, V. R. Leydon, T. J. Miles, N. D. Pearson, R. L. Perera, A. J. Shillings, M. N. Gwynn and B. D. Bax, *Nat. Struct. Mol. Biol.*, 2010, **17**, 1152–1153 and the references therein.
6 I. Turel, J. Kljun, F. Perdih, E. Morozova, V. Bakulev, N. Kasyanenko, J. A. W. Byl and N. Osheroff, *Inorg. Chem.*, 2010, **49**, 10750–10752.
7 S. Badal, Y. F. Her and L. J. Maher III, *J. Biol. Chem.*, 2015, **290**, 22287–22297.

8 M. A. Kohanski, D. J. Dwyer, B. Hayete, C. A. Lawrence and J. J. Collins, *Cell*, 2007, **130**, 797–810.
9 D. E. King, R. Malone and S. H. Lilley, *Am. Fam. Physician*, 2000, **61**, 2741–2748.
10 N. C. Baenziger, *Acta Crystallogr.*, 1986, **C42**, 1505–1509.
11 Z. An, W. Qi and J. Huang, *Acta Crystallogr.*, 2007, **E63**, m2084–m2085.
12 W. Qi, J. Huang and Z. An, *Acta Crystallogr.*, 2008, **E64**, m302.
13 A. A. Soayed, H. M. Refaat and D. A. Noor El-Din, *Inorg. Chim. Acta*, 2014, **421**, 59–66.
14 H. Muslu, A. Golcu, M. Tumer and M. Ozsoz, *J. Coord. Chem.*, 2011, **64**, 3393–3407.
15 M. Patel, D. Gandhi and P. Parmar, *Appl. Organomet. Chem.*, 2011, **25**, 348–355.
16 C. Wen, J. Yang, Z. Zeng, J. Gao and Y. Zheng, *Luminescence*, 2017, **32**, 382–386.
17 F. P. Guengerich, *J. Biol. Chem.*, 2018, **293**, 4603–4605.
18 P. Chellan and P. J. Sadler, *Philos. Trans. R. Soc., A*, 2015, **373**, 20140182.
19 G. Crisponi, V. M. Nurchi, D. Fanni, C. Gerosa, S. Nemolato and G. Faa, *Coord. Chem. Rev.*, 2010, **254**, 876–889.
20 C. E. Elwell, N. L. Gagnon, B. D. Neisen, D. Dhar, A. D. Spaeth, G. M. Yee and W. B. Tolman, *Chem. Rev.*, 2017, **117**, 2059–2107.
21 M. Solioz and J. V. Stoyanov, *FEMS Microbiol. Rev.*, 2003, **27**, 183–195.
22 D. S. Sigman, D. R. Graham, V. D' Aurora and A. M. Stern, *J. Biol. Chem.*, 1979, **254**, 12269–12272.
23 D. M. Perrin, A. Mazumder and D. S. Sigman, *Chem. Rev.*, 1993, **93**, 2295–2316.
24 I. Turel, *Coord. Chem. Rev.*, 2002, **232**, 27–47 and references cited therein.
25 G. Psomas and D. P. Kessissoglou, *Dalton Trans.*, 2013, **42**, 6252–6276.
26 E. Chalkidou, F. Perdih, I. Turel, D. P. Kessissoglou and G. Psomas, *J. Inorg. Biochem.*, 2012, **113**, 55–65.
27 G. Mendoza-Diaz, L. M. R. Martinez-Aguilera and R. Perez-Alonso, *Inorg. Chim. Acta*, 1987, **138**, 41–47.
28 G. Psomas, A. Tarushi, Y. Sanakis, E. K. Efthimiadou, C. P. Raptopoulou and N. Katsaros, *J. Inorg. Biochem.*, 2006, **100**, 1764–1773.
29 E. Y. Bivian-Castro, F. Cervantes-Lee and G. Mendoza-Diaz, *Inorg. Chim. Acta*, 2004, **357**, 349–353.
30 L. Yu, Z. Tang, P. Yi, S. Liu and X. Li, *J. Coord. Chem.*, 2008, **61**, 2961–2967.
31 I. Turel, I. Leban and N. Bukovec, *J. Inorg. Biochem.*, 1994, **56**, 273–282.
32 P. Drevensek, T. Zupancic, B. Pihlar, R. Jerala, U. Kolitsch, A. Plaper and I. Turel, *J. Inorg. Biochem.*, 2005, **99**, 432–442.
33 E. K. Efthimiadou, Y. Sanakis, M. Katsarou, C. P. Raptopoulou, A. Karaliota, N. Katsaros and G. Psomas, *J. Inorg. Biochem.*, 2006, **100**, 1378–1388.
34 P. Zivec, F. Perdih, I. Turel, G. Giester and G. Psomas, *J. Inorg. Biochem.*, 2012, **117**, 35–47.
35 P. Ruiz, R. Ortiz, L. Perello, G. Alzuet, M. Gonzalez-Alvarez, M. Liu-Gonzalez and F. Sanz-Ruiz, *J. Inorg. Biochem.*, 2007, **101**, 831–840.
36 B. Macias, M. V. Villa, I. Rubio, A. Castineiras and J. Borras, *J. Inorg. Biochem.*, 2001, **84**, 163–170.
37 A. Kostelidou, S. Kalogiannis, O. A. Begou, F. Perdih, I. Turel and G. Psomas, *Polyhedron*, 2016, **119**, 359–370.
38 E. K. Efthimiadou, Y. Sanakis, C. P. Raptopoulou, A. Karaliota, N. Katsaros and G. Psomas, *Bioorg. Med. Chem. Lett.*, 2006, **16**, 3864–3867.
39 M. Yang, J. Li and P. R. Chen, *Chem. Soc. Rev.*, 2014, **43**, 6511–6526.
40 E. M. Sletten and C. R. Bertozzi, *Angew. Chem., Int. Ed.*, 2009, **48**, 6974–6998.
41 T. Voelker, F. Dempwolff, P. L. Graumann and E. Meggers, *Angew. Chem., Int. Ed.*, 2014, **53**, 10536.
42 A. L. Noffke, A. Habtemariam, A. M. Pizarro and P. J. Sadler, *Chem. Commun.*, 2012, **48**, 5219–5246.
43 J. J. Soldevila-Barreda, I. Romero-Canelon, A. Habtemariam and P. J. Sadler, *Nat. Commun.*, 2015, **6**, 6582.
44 M. Tomas-Gamasa, M. Martinez-Calvo, J. R. Couceiro and J. L. Mascarenas, *Nat. Commun.*, 2016, **7**, 12538.
45 J. Marmur, *J. Mol. Biol.*, 1961, **3**, 208–211.
46 M. F. Reichmann, S. A. Rice, C. A. Thomas and P. Doty, *J. Am. Chem. Soc.*, 1954, **76**, 3047–3053.
47 Agilent, CrysAlis PRO, Agilent Technologies, Yarnton, Oxfordshire, England, 2011.
48 G. M. Sheldrick, *Acta Crystallogr., Sect. A: Found. Crystallogr.*, 2008, **64**, 112–122.
49 V. A. Blatov, *IUCr CompComm Newsletter*, 2006, **7**, 4–38.
50 V. A. Blatov, A. P. Shevchenko and D. M. Proserpio, *Cryst. Growth Des.*, 2014, **14**, 3576–3586.
51 M. O'Keeffe and O. M. Yaghi, *Chem. Rev.*, 2012, **112**, 675–702.
52 D. Li, M. Li, M. O'Keeffe and O. M. Yaghi, *Chem. Rev.*, 2014, **114**, 1343–1370.
53 (*a*) G. B. Shul'pin, *J. Mol. Catal. A: Chem.*, 2002, **189**, 39–66; (*b*) G. B. Shul'pin, *Mini-Rev. Org. Chem.*, 2009, **6**, 95–104.
54 (*a*) G. B. Shul'pin, *Catalysts*, 2016, **6**, 50; (*b*) G. B. Shul'pin, Y. N. Kozlov, L. S. Shul'pina and P. V. Petrovskiy, *Appl. Organomet. Chem.*, 2010, **24**, 464–472.
55 B. J. Hathaway, in *Comprehensive Coordination Chemistry*, ed. G. Wilkinson, Pergamon Press, Oxford, 1987, vol. 5, pp. 533–773.
56 B. J. Hathaway, *Struct. Bonding*, 1973, **14**, 49–67.
57 A. W. Addison, T. N. Rao, J. Reedijk, J. van Rijn and G. C. Verchoor, *J. Chem. Soc., Dalton Trans.*, 1984, 1349–1356.
58 L. Yu, L. Lai, R. Xia and S. Liu, *J. Coord. Chem.*, 2009, **62**, 1313–1319.
59 (*a*) L. Infantes and S. Motherwell, *CrystEngComm*, 2002, **4**, 454–461; (*b*) M. V. Kirillova, A. M. Kirillov, M. F. C. G. da Silva, M. N. Kopylovich, J. J. R. Fraústo da Silva and A. J. L. Pombeiro, *Inorg. Chim. Acta*, 2008, **361**, 1728–1737; (*c*) Ł. Jaremko, A. M. Kirillov, P. Smoleński and A. J. L. Pombeiro, *Cryst. Growth Des.*, 2009, **9**, 3006–3010.
60 A. M. Kirillov and G. B. Shul'pin, *Coord. Chem. Rev.*, 2013, **257**, 732–755.
61 A. E. Shilov and G. B. Shulpin, *Activation and Catalytic Reactions of Saturated Hydrocarbons in the Presence of Metal Complexes*, Kluwer Acad. Publ., Dordrecht, 2000.

62 G. A. Olah and A. Molnar, *Hydrocarbon Chemistry*, Wiley, 2003.
63 S. Sirajuddin and A. C. Rosenzweig, *Biochemistry*, 2015, **54**, 2283–2294.
64 (*a*) T. A. Fernandes, C. I. M. Santos, V. André, J. Klak, M. V. Kirillova and A. M. Kirillov, *Inorg. Chem.*, 2016, **55**, 125–135; (*b*) M. V. Kirillova, C. I. M. Santos, W. Wu, Y. Tang and A. M. Kirillov, *J. Mol. Catal. A: Chem.*, 2017, **426**, 343–349.
65 (*a*) M. V. Kirillova, C. I. M. Santos, V. André, T. A. Fernandes, S. S. P. Diasa and A. M. Kirillov, *Inorg. Chem. Front.*, 2017, **4**, 968–977; (*b*) S. S. P. Dias, M. V. Kirillova, V. André, J. Klak and A. M. Kirillov, *Inorg. Chem. Front.*, 2015, **2**, 525–537.
66 (*a*) T. A. Fernandes, C. I. M. Santos, V. André, S. S. P. Dias, M. V. Kirillova and A. M. Kirillov, *Catal. Sci. Technol.*, 2016, **6**, 4584–4593; (*b*) S. S. P. Dias, M. V. Kirillova, V. André, J. Klak and A. M. Kirillov, *Inorg. Chem.*, 2015, **54**, 5204–5212; (*c*) T. A. Fernandes, V. André, A. M. Kirillov and M. V. Kirillova, *J. Mol. Catal. A: Chem.*, 2017, **426**, 357–367.
67 (*a*) G. B. Shul'pin, *Dalton Trans.*, 2013, **42**, 12794–12818; (*b*) G. B. Shul'pin, *Org. Biomol. Chem.*, 2010, **8**, 4217–4228.
68 (*a*) S. Gupta, M. V. Kirillova, M. F. C. G. da Silva, A. J. L. Pombeiro and A. M. Kirillov, *Inorg. Chem.*, 2013, **52**, 8601–8611; (*b*) M. V. Kirillova, A. M. Kirillov and A. J. L. Pombeiro, *Chem. – Eur. J.*, 2010, **16**, 9485–9493; (*c*) M. V. Kirillova, A. M. Kirillov and A. J. L. Pombeiro, *Adv. Synth. Catal.*, 2009, **351**, 2936–2948; (*d*) M. V. Kirillova, A. M. Kirillov, M. L. Kuznetsov, J. A. L. Silva, J. J. R. Frausto da Silva and A. J. L. Pombeiro, *Chem. Commun.*, 2009, 2353–2355; (*e*) A. M. Kirillov, M. Haukka, M. F. C. G. da Silva and A. J. L. Pombeiro, *Eur. J. Inorg. Chem.*, 2005, 2071–2080; (*f*) A. M. Kirillov, J. A. S. Coelho, M. V. Kirillova, M. F. C. G. da Silva, D. S. Nesterov, K. R. Gruenwald, M. Haukka and A. J. L. Pombeiro, *Inorg. Chem.*, 2010, **49**, 6390–6392.
69 I. Tsitsa, A. Tarushi, P. Doukoume, F. Perdih, A. de Almeida, A. Papadopoulos, S. Kalogiannis, A. Casini, I. Turel and G. Psomas, *RSC Adv.*, 2016, **6**, 19555–19570.
70 E. K. Efthimiadou, M. E. Katsarou, A. Karaliota and G. Psomas, *J. Inorg. Biochem.*, 2008, **102**, 910–920.
71 V. Uivarosi, *Molecules*, 2013, **18**, 11153–11197.
72 A. D. Russell, in *Disinfection, Sterilization and Preservation*, ed. S. S. Block, 4th edn, Lea and Febinger, Philadelphia, 1991, pp. 27–59.
73 H. W. Rossmore, in *Disinfection, Sterilization and Preservation*, ed. S. S. Block, 4th edn, Lea and Febinger, Philadelphia, 1991, pp. 290–321.
74 J. R. Lakowicz, *Principles of Fluorescence Spectroscopy*, third edn, Plenum Press, New York, 2006.
75 C. Tan, J. Liu, H. Li, W. Zheng, S. Shi, L. Chen and L. Ji, *J. Inorg. Biochem.*, 2008, **102**, 347–358.
76 G. Zhao, H. Lin, S. Zhu, H. Sun and Y. Chen, *J. Inorg. Biochem.*, 1998, **70**, 219–226.
77 V. Rajendiran, R. Karthik, M. Palaniandavar, H. Stoeckli-Evans, V. S. Periasamy, M. A. Akbarsha, B. S. Srinag and H. Krishnamurthy, *Inorg. Chem.*, 2007, **46**, 8208–8221.
78 O. H. Laitinen, V. P. Hytonen, H. R. Nordlund and M. S. Kulomaa, *Cell. Mol. Life Sci.*, 2006, **63**, 2992–3017.
79 M. M. Aleksic and V. Kapetanovic, *Acta Chim. Slovaca*, 2014, **61**, 555–573.
80 B. M. Zeglis, V. C. Pierre and J. K. Barton, *Chem. Commun.*, 2007, 4565–4579.
81 Q. Zhang, J. Liu, H. Chao, G. Xue and L. Ji, *J. Inorg. Biochem.*, 2001, **83**, 49–55.
82 A. Wolfe, G. Shimer and T. Meehan, *Biochemistry*, 1987, **26**, 6392–6396.
83 J. L. Garcia-Gimenez, M. Gonzalez-Alvarez, M. Liu-Gonzalez, B. Macias, J. Borras and G. Alzuet, *J. Inorg. Biochem.*, 2009, **103**, 923–934.
84 W. D. Wilson, L. Ratmeyer, M. Zhao, L. Strekowski and D. Boykin, *Biochemistry*, 1993, **32**, 4098–4104.
85 E. K. Efthimiadou, N. Katsaros, A. Karaliota and G. Psomas, *Inorg. Chim. Acta*, 2007, **360**, 4093–4102.
86 A. Bykowska, U. K. Komarnicka, M. Jeżowska-Bojczuk and A. Kyziol, *J. Inorg. Biochem.*, 2018, **181**, 1–10.
87 J. R. Stone and S. Yang, *Antioxid. Redox Signaling*, 2006, **8**, 243–270.
88 U. Schuchardt, D. Cardoso, R. Sercheli, R. Pereira, R. S. Cruz, M. C. Guerreiro, D. Mandelli, E. V. Spinace and E. L. Pires, *Appl. Catal., A*, 2001, **211**, 1–17.

